Fractures modeling in system of engineering analysis

A.Yu. Babin

FSBEI HE «Ufa State Petroleum Technological
University», Ufa, Russia
aubabin@yandex.ru

V.A. Gafarova

FSBEI HE «Ufa State Petroleum Technological
University», Ufa, Russia
gafarova.vika@bk.ru

V.K. Berdin

FSBEI HE «Ufa State Petroleum Technological
University», Ufa, Russia
berdinvk@mail.ru

Abstract—**Equipment used at the enterprises implementing oil and gas technologies is potentially hazardous and should be of high degree of reliability. Reliability of equipment reduces the number of defects appearing during the operation process. One of hazardous and unpredictable defects is fracture. If there is a fracture, it is permitted to operate an installation under operating conditions up to the definite critical size of the fracture. However, to operate the installation with fracture, it is required to perform a detailed study of the defect and to calculate residual operation life of the equipment. One of the most suitable methods of fracture studying is finite element analysis. The article presents the method of fractures modeling in the system of engineering analysis, ANSYS, and comparison of obtained results with analytical solution.**

Keywords—oil refineries, oil and gas technologies, defect, fracture, modeling, system of engineering analysis, stress intensity factor.

I. INTRODUCTION

Equipment implementing oil and gas technologies operates under conditions of thermal force impact, cycling loads, instability of operating parameters. Taking into account that this equipment have large dimensions, it could be noted that a great number of fire and explosion hazard and toxic substances are in a limiting state per unit time [1].

Equipment reliability reduces the number of defects appearing during the operation process. One of the hazardous and unpredictable defects is fracture. For certain types of equipment, operation under operating conditions up to the definite critical size of the fracture is acceptable [2].

It should be noted that provision of equipment safety is based on the concept of destruction control, which lies in the fact that defects are always present, even in new structures [3].

II. MAIN PART

Possibility of operating equipment with fractures comes from the availability of critical size of fractures, up to the achievement of which the fractures is in latent state. In order to determine critical fracture length (a), it is necessary to know the value of stress intensity factor $K = (N/m^{3/2})$ [4]:

$$K_I = \sigma\sqrt{\pi a}, \tag{1}$$

where σ – critical mechanical stress, MPa.

Destruction occurs when stress in the construction material with fracture of the length (a) reaches critical value $\sigma_{cr.}$ In such case:

$$K_I = \sigma_{cr}\sqrt{\pi a} = K_c, \tag{2}$$

being K_c – characteristic of the material.

When detecting fracture by means of nondestructive control performance or visual examination of the equipment, it is necessary to assess the critical size of defects and make decision regarding the possibility of its further operation [3].

When making such decision, it is necessary to take into account possible change of K_c value in the process of damages accumulation. In his paper, Kuzeev M.I. shows that in case of fatigue loading of steel samples in the low-cycle area as per the pure bending scheme, under the general tendency for the K_c decrease, extreme values are observed when achieving 30 % and 70 % of the number of cycles to the complete failure.

These results point to the high-risk level when operating equipment with fractures. Reduction of the risk level is possible by filling the fracture cavity with the composition material consisting of various fillers by means of using special device [5].

Multivariance of change in construction material characteristics during the operation process, the type of

interaction with the composition material requires performance of multiple calculations to assess fracture behavior in the construction. Such task could be fulfilled by means of carrying out studies on three-dimensional models by the finite elements method (FEM) [6].

Software package ANSYS was used for this purpose. At the first stage of studies, the flat plate with edge through-fracture of l length was simulated (figure 1).
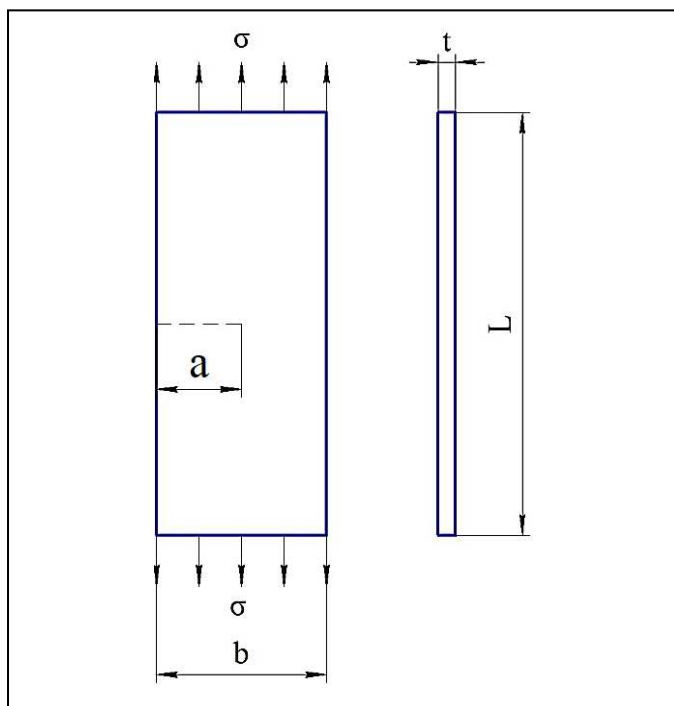
Fig. 1. Flat plate with edge through-fracture

Fracture modeling in the system of engineering analysis ANSYS is performed by means of the eXtended Finite Element Method (hereinafter referred to as the XFEM). This method proposes a suitable engineering approach for fractures modeling, not involving FE mesh reconstruction in the field of fracture development. The method of fractures modeling based on XFEM also can be applied for fatigue fractures growth modeling [7].

Fracture modeling in MAPDL is more suitable to perform by entering the required commands in the command line. The whole process of modeling could be divided into two stages listed in table 1.

TABLE I.   PROCEDURE OF FRACTURE MODELING IN MAPDL

Stage of modeling	Command
Selection of the FE type	Et; keyopt
Determination of material properties	mp, ex (E); mp, nuxy (μ); mp, dens (ρ)
Creation of points in the selected system of coordinates	K
Determination of the field of elements (figure 2)	A
Determination of FE size	Lsel; lesize (line division to FE)
Creation of FE mesh (figure 3)	Esize (FE size); amesh
Uniting FE into group	Cm
Determination of FE which will take part in XFEM method	Xfenrich
Fracture placement (figure 3)	Xfdata
Provision of boundary conditions	Press (pressure); d (joint constraint)
Determination of the solution parameters	Cint
Displaying of the solution results	Prcint

The ANSYS system does not use some definite measuring system, that is why, entered data should be comparable (table 2) [7].

TABLE II.   SELECTED MEASURING UNITS

Parameter	Measuring unit
Length	mm, millimeter
Power	N, Newton
Weight	t, tonne
Time	s, second
Mechanical stress	MPa (N/mm^2)
Density	t/mm^2

Sample geometrical dimensions and testing parameters are provided in table 3.

TABLE III.   SAMPLE GEOMETRICAL DIMENSIONS AND TESTING PARAMETERS

Parameter	Fracture length, mm	Sample geometry, mm			Tensile stress, MPa
	a	*b*	*h*	*t*	*σ*
Value	20	40	200	4	100

Material properties are specified for steel 09G2S:

- density $\rho = 7.85 \cdot 10^{-9}$ t/mm^3 (7850 kg/m^3);

- module of elasticity $E = 2 \cdot 10^5$ MPa;

- Poisson ratio $\mu = 0.3$.

Let us complete the set task in the following schemes of the stressed-deformed state:

- 2D, the plain deformation state (hereinafter referred to as the PDS) in Mechanical APDL (hereinafter MAPDL);

- 2D, plain stress state (hereinafter PSS) in MAPDL;

- 3D in ANSYS Workbench (hereinafter WB).

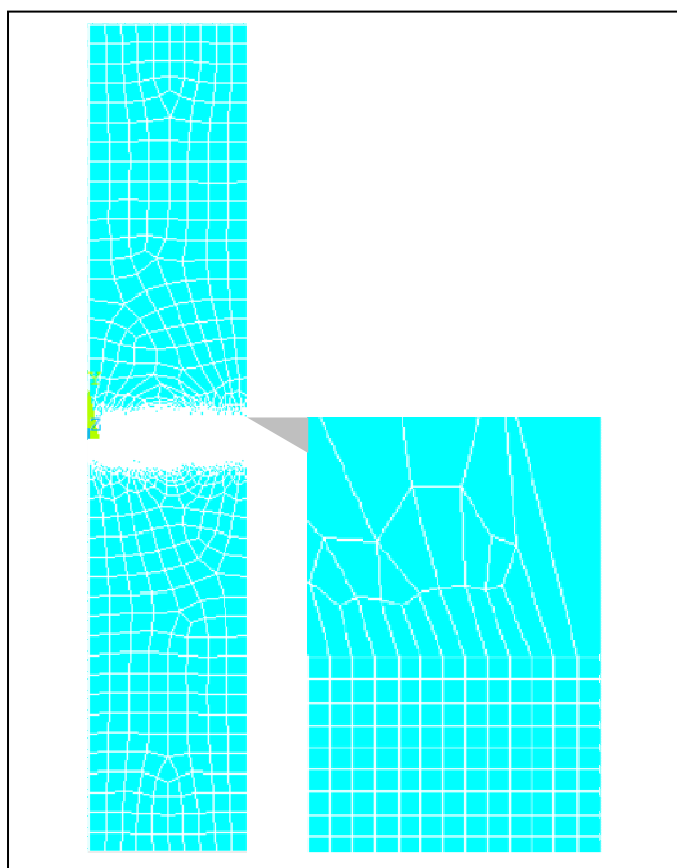The fracture model developed in MAPDL is presented in figures 2, 3.
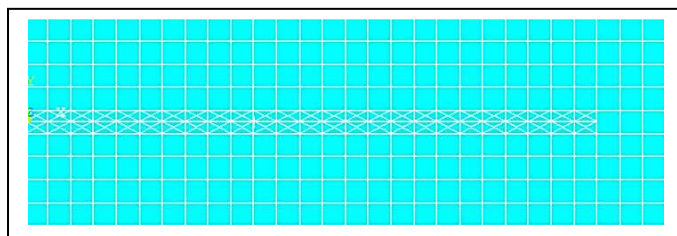
b.

Fig. 2. FE mesh

c.

Fig. 3. Fracture simulated by XFEM method

ANSYS Workbench by means of commands in Fracture inset prevents through fracture modeling. That is why, it was decided to artificially implement in the plate the fracture of such geometry, angle between the edges, at the apex of which it will not depend on the fracture depth (figure 4).

Distribution of equivalent stresses obtained in Mechanical APDL and ANSYS Workbench at the apex of fracture is illustrated in figure 5.
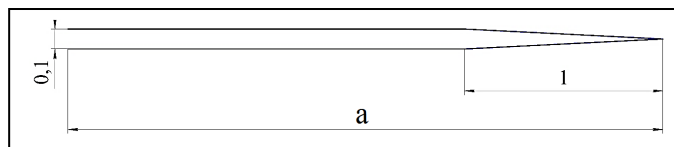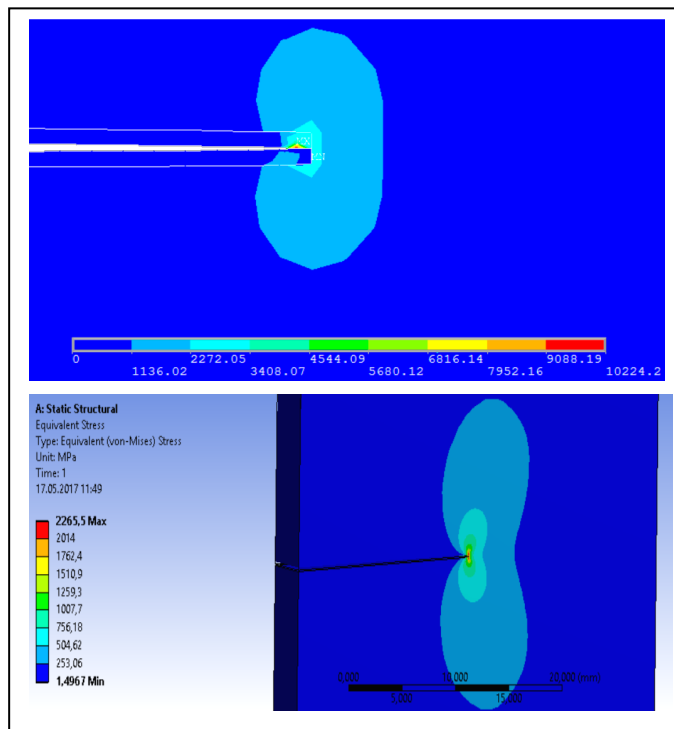
d.

Fig. 4. Fracture dimensions

e.

Fig. 5. Diagram of equivalent stresses distribution, MPa

Moreover, ANSYS Workbench allows displaying the calculation result of the K_I factor along the fracture length (figure 6).
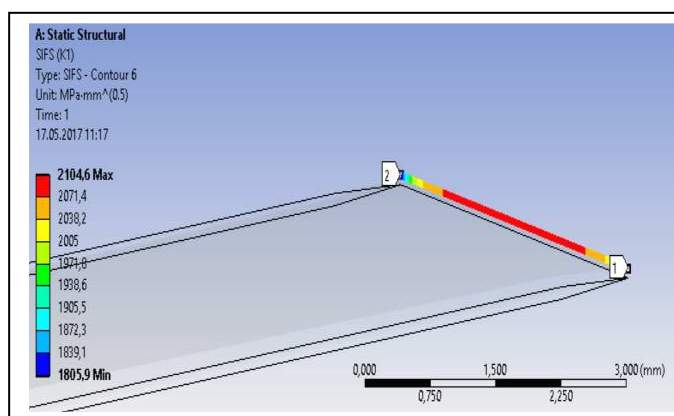
f.

Fig. 6. Diagram of K_I distribution on fracture front, MPa·mm$^{0.5}$

To determine dependence of fracture length a and stress intensity factor K_I for the I-st type of loading [8], the process of extension of the flat plate with through-fracture of the length $1 \leq a \leq 39$ mm was simulated.

To assess results of fracture modeling, it was decided to compare results of K_I calculation, obtained in ANSYS, with the results, obtained from the analytical method. Let us analytically solve the task by using formulas specified in GOST 25.506-85 [9] (hereinafter GOST) and in the reference book [10].

In accordance with GOST for the flat plate with edge through-fracture, K_I in a wide range of fracture lengths ($0 \leq \lambda \leq 0.6$), bing $\lambda = a/b$, is calculated by the formula:

$$K_I = \frac{P\sqrt{a}}{t \cdot b} Y_5, \qquad (3)$$

where, $Y_5 = 1.99 - 0.41\dfrac{1}{b} + 18.7\left(\dfrac{1}{b}\right)^2 - 38.48\left(\dfrac{1}{b}\right)^3 + 53.85\left(\dfrac{1}{b}\right)^4$.

In accordance with the reference book [10], K_I under condition of $0 \leq \lambda \leq 0.6$ is calculated by the formula:

$$K_I = \sigma\sqrt{\pi a} \cdot F_I(\lambda), \qquad (4)$$

where, $F_I(\lambda) = 1.12 - 0.231\lambda + 10.55(\lambda)^2 - 21.72(\lambda)^3 + 30.39(\lambda)^4$.

In order to verify, let us compare results of K_I, obtained in ANSYS, with the results, calculated by analytical method (table 4). Graphic representation of the results is provided in figure 7.
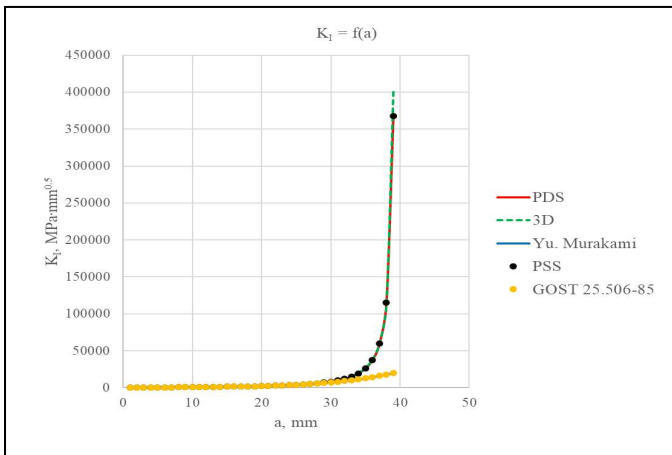
g.

Fig. 7.   Comparison of results obtained by all mentioned methods

The graph shows that good repeatability of K_I values is observed within the interval of fracture lengths from 0 up to 24 mm, which makes 60 % of the total width of the sample. Thereafter values obtained in ANSYS and results of analytical method differ.

Let us determine the function which provides the most precise $K_I = f(a)$ dependence. Analyzing the obtained results, it was found out that $K_I = f(a)$ dependence is unstable in the

fracture lengths range. The most monotonic behavior is observed within the intervals $0 \leq \lambda \leq 60\%$ and $60\% \leq \lambda \leq 100\%$.

The interval of $K_I = f(a)$ dependence in case of $0 \leq \lambda \leq 60\%$ is most accurately described by the third-order polynom (figure 8):

$$K_I = y_0 + b \cdot a + c \cdot a^2 + d \cdot a^3, \qquad (5)$$

where $y_0 = 81.7874;$

$b = 108.5224;$

$c = -6.7414;$

$d = 0.3382.$

TABLE IV. K_I VALUES OBTAINED BY ANALYTICAL METHOD AND IN ANSYS SYSTEM

l, mm	K_I, MPa·mm^2				
	GOST 25.506-85	Yu. Murakami	PDS	PSS	3D
1	199.1	198.6	200.1	200.1	193.9
2	284.5	283.8	285.3	285.1	293.6
3	355.1	354.1	354.7	354.1	368.1
4	420.6	419.5	419.1	417.9	436.1
5	485.0	483.8	482.1	480.4	501.4
6	550.3	549.0	546.3	544.1	569.7
7	617.8	616.4	612.3	609.5	639.1
8	688.5	687.0	681.5	678.4	712.0
9	763.2	761.6	755.1	751.5	789.6
10	842.9	841.1	833.9	830.2	872.9
11	928.4	926.5	920.1	916.5	962.6
12	1020.9	1018.9	1014.7	1011.4	1060.5
13	1122.0	1119.8	1120.1	1117.0	1167.8
14	1233.1	1230.8	1224.7	1222.1	1285.0
15	1356.2	1353.8	1349.1	1346.9	1415.4
16	1493.5	1491.0	1487.4	1485.1	1559.8
17	1647.7	1645.0	1641.8	1638.8	1720.6
18	1821.8	1818.9	1817.0	1813.0	1901.2
19	2018.9	2015.9	2013.2	2008.1	2104.6
20	2243.1	2239.8	2237.9	2231.9	2335.2
21	2498.3	2494.8	2493.2	2486.3	2598.6
22	2789.3	2785.6	2786.1	2778.7	2899.9
23	3121.1	3117.2	3123.6	3116.0	3249.2
24	3499.5	3495.3	3521.1	3513.4	3656.7
25	3930.4	3926.0	3994.5	3987.2	4128.2
26	4420.5	4415.8	4565.6	4558.2	4705.9

27	4976.9	4971.9	5172.8	5165.8	5392.1
28	5607.3	5602.0	5976.1	5971.1	6230.9
29	6319.9	6314.3	6971.4	6966.9	7270.8
30	7123.7	7117.7	8221.6	8214.4	8585.9
31	8027.9	8021.6	9857.6	9847.3	10286.0
32	9042.6	9035.9	12047.0	12034.0	12549.0
33	10178.4	10171.3	15087.0	15071.0	15667.0
34	11446.6	11439.1	19480.	19462.0	20169.0
35	12859.0	12851.1	26268.0	26245.0	27076.0
36	14428.2	14419.8	37654.0	37624.0	38605.0
37	16167.4	16158.5	59659.0	59613.0	60537.0
38	18090.5	18081.0	115220.0	115120.0	112830.0
39	20211.9	20201.9	367690.0	367910.0	402090.0

h.

i.

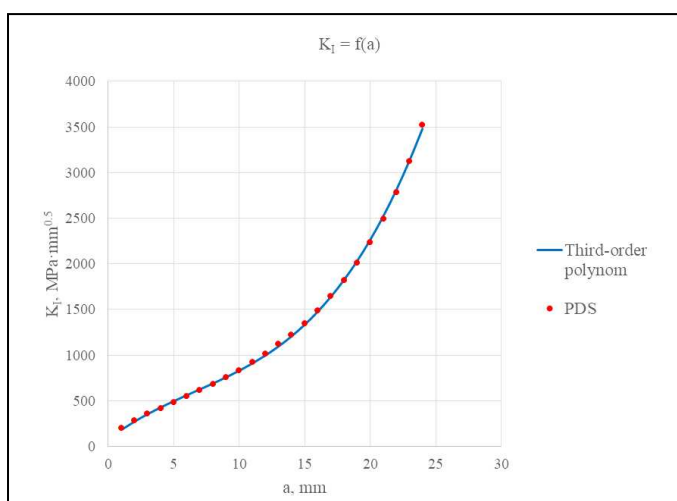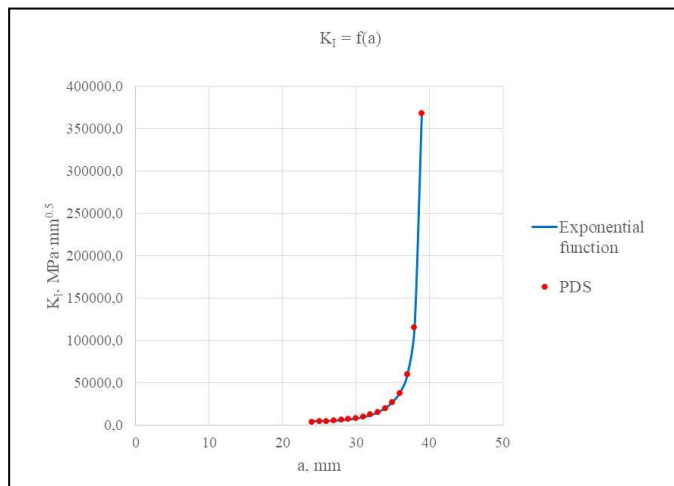Fig. 9. Comparison of results obtained in MAPDL and by means of function in interval of $60 \le \lambda \le 100\%$

Fig. 8. Comparison of results obtained in MAPDL and by means of function in interval of $0 \le \lambda \le 60\%$

The interval of $K_I = f(a)$ dependence in case of $60\% \le \lambda \le 100\%$ is most accurately described by the exponential function (figure 9):

$$K_I = y_0 + b \cdot e^{c \cdot a} + d \cdot e^{g \cdot a}, \qquad (6)$$

where $y_0 = 3920.1834$;

$\qquad a = 0.0634$;

$\qquad b = 0.3658$;

$\qquad c = 3.3678 \cdot 10^{-26}$;

$\qquad d = 1.8241$.

During the next stage of study, 09G2S steel samples with a fracture were destructed on the static and cyclic tests unit Instron 8801. Samples before and after destruction are shown in Figures 10, 11.

j.

Fig. 10. 09G2S steel sample before destruction

Fig. 11. 09G2S steel sample after destruction

III. DISCUSSION

Analysis of the break nature shows that implementation of large plastic deformations was required to advance the fracture. As it is shown by experiments and stress design analysis in the fracture area [11,12], the real critical fracture size, which may increase, can be quite large. Since stresses at the fracture tip exceed the yield strength, the fracture can grow under nominal stresses realized in the elastic area. Singularity of stresses at the fracture tip reduces the accuracy of determining the critical stress coefficient K_{IC} and, as a consequence, the accuracy of the critical fracture length determination. Therefore, a more reliable way of evaluation of the structural material fracture resistance is the use of the critical deformation intensity factor [13].

IV. CONCLUSION

After analyzing the obtained results, one can make the following conclusions:

• Error of K_I results obtained in the system of engineering analysis ANSYS MAPDL and by the analytical method (as per GOST) within the range of formula applicability ($\lambda \leq 0.6$) is less than 1 % and starts to grow when the fracture length exceeds 24 mm. That corresponds to $\lambda = 0.6$. In this connection, the authors can make the conclusion that it is practical and reasonable to solve problems of fracture mechanics in MAPDL.

• Difference of results, obtained in MAPDL and in WB, is almost constant and is less than 5 %. In this connection, the authors conclude that this error resulted from the difference in fracture geometry; thus, solving fracture mechanics problems in WB is also possible.

• For real structures, the obtained design factors should be used for calculation of deformation intensity factors.

References

[1] "On the industrial safety of hazardous production facilities (as amended on March 7. 2017) (edition came into force starting from March 25. 2017)," Federal Law of the Russian Federation № 116-FL. Art. 2.1.

[2] ASME B31G, "Manual for Determining the Remaining Strength of Corroded Pipelines."

[3] J.A. Collins, "Failure of materials in mechanical design," New York, 1981.

[4] M.F. Ashly, D.R.H. Jones, "Engineering Materials I: An Introduction to Properties. Applications and Design. Therd Edition," Pergamon Press, Oxford, 2005.

[5] R.R. Tlyasheva, V.A. Gafarova, K.R. Vagazova, A.M. Kuzeev, "Composition material for filling fracture cavity and fracture-like defects," Bashkir chemical journal, vol. 23, No. 3, p.p. 56-62, 2016.

[6] L. Xue, G.E.O. Widera, Z.F. Sang, "Influence of pad reinforcement on the limit and burst pressures of a cylinder-cylinder intersection," Journal of Pressure Vessel Technology, vol. 125, No. 2, p.p. 182-187, 2003.

[7] ANSYS Help. 2016 [electronic source] URL: https://www.sharcnet.ca/Software/Ansys/16.2.3/en-us/help/ans_frac/.html (16.05.2017 г.).

[8] J. Rosler, H. Harders, M. Baker, "Mechanidchers Verhalten der Werkstoffe," Vieweg+Teubner. GWV Fachverlage GmbH. Wiesbadeb, 2008

[9] GOST 25.506-85, "Strength calculations and testing. Methods of metals mechanical testing. Determination of fracture resistance (fracture viscosity) characteristics under conditions of static loading," Interstate standard, 38 p, 1986.

[10] Y. Murakami, "Stress intensity factor handbook," The Society of Materials Science, vol. 2, Japan, 1987.

[11] R.S. Zaynullin, E.M. Morozov, A.A Aleksandrov, "Criteria of safe destruction of pipeline systems elements with fractures," Nauka, 2005, 316 p.

[12] A.A. Shaniavsky, "Safe fatigue destruction of airframe elements. Synergetics in engineering applications," Ufa, 2003, 803 p.

[13] N.A. Makhutov, "Structural strength, service life and anthropogenic safety: In 2 parts," Novosibirsk: Nauka, 2005. Part 1: Criteria of strength and service life, 494 p.; Part 2: Justification of service life and safety, 610 p.